

Holistic Calculation of (Multi)-Chambered ETFE-Cushions

Dr. Dieter Ströbel, Dr. Peter Singer and Jürgen Holl

technet GmbH gründig + partner, Pestalozzistr. 8, 70563 Stuttgart, Germany

Abstract

Formfinding, statical analysis and cutting pattern generation are considered with respect to a holistic statical calculation; it means, that a complete model is analysed under external loadings by taking into consideration e.g. the gas-laws for several chambers and simultaneously any boundary conditions (as bending stiff beam-elements).

Extended formfinding theories are presented firstly; the extension of the well-known force density method by additional conditions (volume or inner pressure) to a so-called volume formfinding is described. Examples for single- and multi-chambered (volume-) formfinding projects are shown.

Statical Analysis of the structures is a problem in case of a holistic formulation. The isotropic material behavior of ETFE-foils is described by two values (E-modulus and Poisson's ratio); the constitutive equations rule the relationship between stress and strain and here we need 4 stiffness values, which are calculated from the already mentioned material values for ETFE. To calculate pneumatic systems with known internal pressure values is not possible in all load-case situations. E.g. under fast wind gusts the gas law has to be used; it means the product from volume and internal pressure remains constant in the chambers during loading. In many cases the chambered cushions are fixed to a bending stiff (steel) boundary. The deflections of these steel-elements under loads cannot be neglected and therefore they have to be part of the structural (holistic) system.

Patterning of ETFE-cushions has to be made with highest accuracy: the reason is because of the material itself and also because of the fixed boundaries. We support the engineers by quality numbers of the patterning. In case of many cushions for big

project mass production has to be applied: in order to manage it automatic patterning tools are presented briefly.

Keywords: [ETFE, pneumatic cushions, formfinding, static Analysis, patterning]

1 Formfinding of Pneumatics

The theory of the Formfinding of pneumatic cushions has its basics in the well-known Force-Density Method ([1], [2] and [3]). The Force-Density Method creates a linear system of equations for the form-finding procedure by defining the ratio between Force S and stressed length l to be known. Hereby the nonlinear equations of the equilibrium change to a linear system.

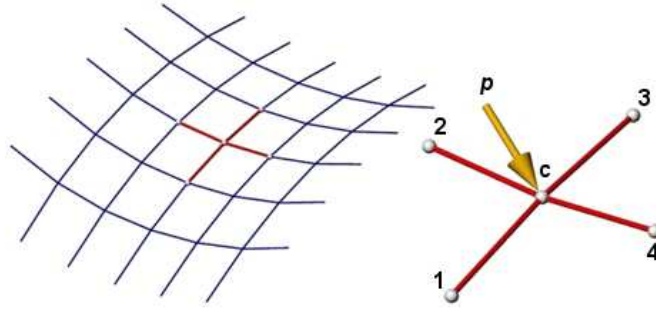


Figure 1: Four cables in point C

In order to clarify these facts *Fig. 1* shows a point C which is connected by cables to 4 points (1,2,3,4). The nonlinear equations of the equilibrium in the point C are as follows, where the external load-vector can be expressed $\mathbf{p}^t = (p_x \ p_y \ p_z)$.

$$\begin{aligned} (x_c - x_1) \frac{S_1}{l_1} + (x_c - x_2) \frac{S_2}{l_2} + (x_c - x_3) \frac{S_3}{l_3} + (x_c - x_4) \frac{S_4}{l_4} &= p_x \\ (y_c - y_1) \frac{S_1}{l_1} + (y_c - y_2) \frac{S_2}{l_2} + (y_c - y_3) \frac{S_3}{l_3} + (y_c - y_4) \frac{S_4}{l_4} &= p_y \\ (z_c - z_1) \frac{S_1}{l_1} + (z_c - z_2) \frac{S_2}{l_2} + (z_c - z_3) \frac{S_3}{l_3} + (z_c - z_4) \frac{S_4}{l_4} &= p_z \end{aligned}$$

These equations become linear by assuming known force-densities, e.g. $q_1 = \frac{S_1}{l_1}$,

and analogue for q_2, q_3 and q_4 . The force-density equations are as follows:

$$\begin{aligned} (x_c - x_1)q_1 + (x_c - x_2)q_2 + (x_c - x_3)q_3 + (x_c - x_4)q_4 &= p_x \\ (y_c - y_1)q_1 + (y_c - y_2)q_2 + (y_c - y_3)q_3 + (y_c - y_4)q_4 &= p_y \\ (z_c - z_1)q_1 + (z_c - z_2)q_2 + (z_c - z_3)q_3 + (z_c - z_4)q_4 &= p_z \end{aligned}$$

The coordinates of the point C are the solution of these linear equations. In the following step we want to write the above system by considering m neighbors in the point C :

$$\begin{aligned} \sum_{i=1}^m (x_i - x_c) q_i - p_x &= 0 \\ \sum_{i=1}^m (y_i - y_c) q_i - p_y &= 0 \\ \sum_{i=1}^m (z_i - z_c) q_i - p_z &= 0 \end{aligned} \quad (1)$$

The energy which belongs to the system (1) can be written as (see also [4] and [5])

$$\Pi = \frac{1}{2} \mathbf{v}^t \mathbf{R} \mathbf{v} - p_x (x - x_0) - p_y (y - y_0) - p_z (z - z_0) \Rightarrow stat.$$

The internal energy is the expression $\frac{1}{2} \mathbf{v}^t \mathbf{R} \mathbf{v}$. The vector $\mathbf{v}^t = (v_x \quad v_y \quad v_z)$ and the matrix $\mathbf{R} = diag(q_i \quad q_i \quad q_i)$ show this energy with respect to a single line element i . We can write the inner energy as $\frac{1}{2} q_i (v_x^2 + v_y^2 + v_z^2)$, precisely:

$$\begin{aligned} v_x &= x_i - x_c \\ v_y &= y_i - y_c \\ v_z &= z_i - z_c \end{aligned} \quad \mathbf{R} = \begin{bmatrix} q_i & 0 & 0 \\ & q_i & 0 \\ sym. & & q_i \end{bmatrix}$$

The chamber of a pneumatic cushion has a volume V , which is made by an internal pressure p_i . The product from internal pressure and volume is a part of the total energy Π : a given volume V_0 leads directly to a specific internal pressure p_i : hence the total energy for the formfinding of a pneumatic cushion is

$$\Pi = \frac{1}{2} \mathbf{v}^t \mathbf{R} \mathbf{v} - p_x (x - x_0) - p_y (y - y_0) - p_z (z - z_0) - p_i (V - V_0) \Rightarrow stat.$$

The derivation of the total energy to the unknown coordinates and to the unknown internal pressure ends up with

$$\begin{aligned}
\frac{\partial \Pi}{\partial x} &= \sum_{i=1}^m (x_i - x_c) q_i - p_x - p_i \frac{\partial V}{\partial x} = 0 \\
\frac{\partial \Pi}{\partial y} &= \sum_{i=1}^m (y_i - y_c) q_i - p_y - p_i \frac{\partial V}{\partial y} = 0 \\
\frac{\partial \Pi}{\partial z} &= \sum_{i=1}^m (z_i - z_c) q_i - p_z - p_i \frac{\partial V}{\partial z} = 0 \\
\frac{\partial \Pi}{\partial p_i} &= V - V_0 = 0
\end{aligned} \tag{2}$$

In the system (2) the internal pressure p_i can be seen as a so-called Lagrange multiplier. The fourth column in (2) shows, that our boundary condition $V = V_0$ is obtained by the derivation of the energy to this Lagrange multiplier. The vector $(\frac{\partial V}{\partial x} \quad \frac{\partial V}{\partial y} \quad \frac{\partial V}{\partial z})$ describes the normal direction in the point (x, y, z) and the size is the according area. By a set of given force-densities for all elements and also a given volume V_0 we end up with a pre-stressed and of course balanced pneumatic system with a volume V_0 and an internal pressure p_i .

Each additional chamber leads to an additional Volume and Lagrange multiplier, which allows to calculate multi-chambered cushions (see Fig.2).

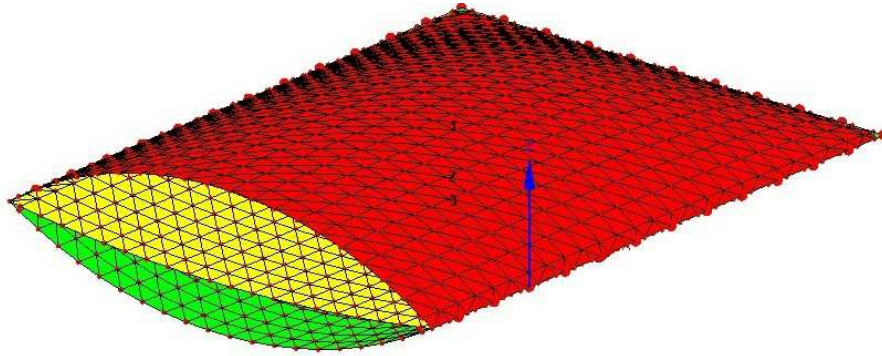


Figure 2: 2 chambers with 3 layers.

The force-densities q and the internal pressure p_i are not independent from each other. We are going to show it with the following single-chamber-example.

Example 1:

The Volume Formfinding example has the geometry 20 m by 10 m . The required volume V_0 of a single chambered-cushion is 400 m^3 . A stress distribution of 1 kN/m in both directions leads to an internal pressure of 0.16 kN/m^2 . The sag is 1.95 m .

Although the engineer likes this result with respect to its geometry, it may happen that he wants to get a higher internal pressure as operating pressure (e.g. 0.35 kN/m^2). In this case he simply has to use a higher pre-stress $0.35 / 0.16 * 1 \text{ kN/m} = 2.1875 \text{ kN/m}$ in order to get the desired pressure of 0.35 kN/m^2 . The geometry remains unchanged.

The rule is: the stresses are proportional to the internal pressure. So we notice $\sigma \approx p_i$ in case of non-changing geometry in the Volume Formfinding procedure.

We want to point out again, that in the Volume Formfinding no material properties are used, only force-densities in all elements and a desired volume are inputted and then we receive the form by solving system (2). Usually the additional external loads (p_x, p_y, p_z) do not exist.

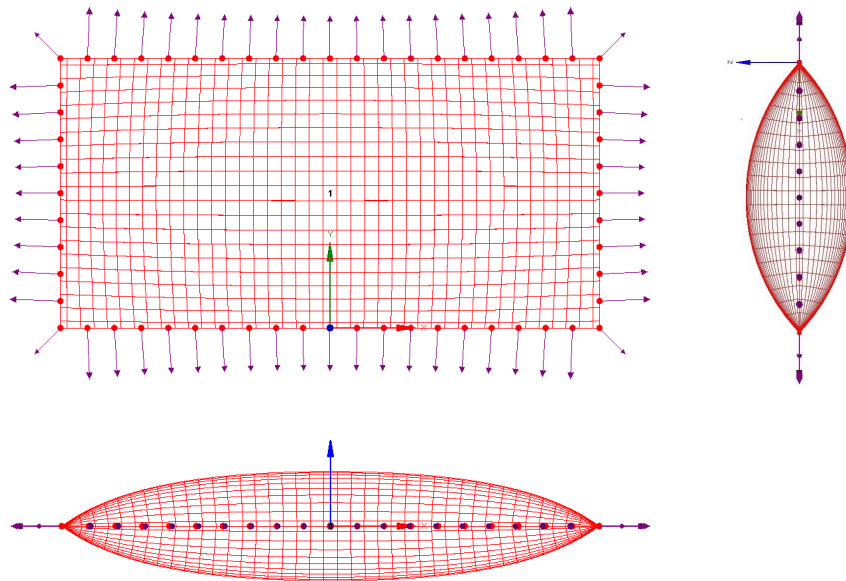


Figure 3: Pneumatic chamber

2 Statical Analysis of Pneumatics

Membrane Elements

We extend the form-finding theory by introducing the constitutive equations for the membrane elements to the system (1). Now the force-densities q from the form-finding are unknowns and they belong to the material equations.

$$\begin{bmatrix} \sigma_u \\ \sigma_v \\ \tau \end{bmatrix} = \begin{bmatrix} m_{11} & m_{12} & 0 \\ & m_{22} & 0 \\ \text{sym.} & & m_{33} \end{bmatrix} \begin{bmatrix} \varepsilon_u \\ \varepsilon_v \\ \Delta\gamma \end{bmatrix}$$

We have to consider, that the membrane axial-stress in u - or v - direction can be expressed as $\sigma_u = \frac{S_u}{b_u}$ and $\sigma_v = \frac{S_v}{b_v}$. b_u and b_v are the widths of the u - and v -

lines. The force-densities q can be introduced now as: $S_u = q_u l_u$ and $S_v = q_v l_v$. The strains in u - and v -direction can be written as follows:

$$\varepsilon_u = \frac{l_u - l_{u0}}{l_{u0}} \quad \text{and} \quad \varepsilon_v = \frac{l_v - l_{v0}}{l_{v0}}. \quad \text{The angle difference } \Delta\gamma = \gamma - \gamma_0 \text{ is needed}$$

for the shear-stress calculation. γ is the angle between u and v -direction; γ_0 refers to the ‘non-deformed start-situation’ without any shear-stress.

The geometrical compatibility has to be considered as follows:

$$l_i = \sqrt{(x_i - x_c)^2 + (y_i - y_c)^2 + (z_i - z_c)^2} \quad \text{and} \quad \gamma = \arccos\left(\frac{l_u * l_v}{l_u l_v}\right), \quad \text{in}$$

which $(l_u * l_v)$ means the inner (scalar-) product between u and v -direction.

The shear-stress calculation is guaranteed also for a continuous membrane by the fact that the shear angle is between the non-deformed u - and v -direction of the material [4].

Now we show an example in *Fig. 3* with isotropic material (e.g. ETFE 200 μm) which is given by only an E -modulus and Poisson’s ratio ν . With $E = 180 \text{ kNm}^{-1}$ and $\nu = 0.33$ we receive the relations

$$\begin{bmatrix} m_{11} & m_{12} & 0 \\ & m_{22} & 0 \\ \text{sym.} & & m_{33} \end{bmatrix} = \frac{E}{1 - \nu^2} \begin{bmatrix} 1 & \nu & 0 \\ & 1 & 0 \\ \text{sym.} & & (1 - \nu)/2 \end{bmatrix} = \begin{bmatrix} 202 & 67 & 0 \\ & 202 & 0 \\ \text{sym.} & & 67 \end{bmatrix}$$

in the units kNm^{-1} . After having introduced this material properties we calculate 3 load cases, showing the different possibilities in ‘Volume Statical Analysis’.

LC 1: Permanent Snow Load (steered by a fixed inner pressure ($p_i=p_{fixed}$))

The snow loads are only on the top-layer of the cushion. The operating pressure is increased in winter from 0.35 kN/m^2 to 1.00 kN/m^2 under a large permanent snow load of 0.9 kN/m^2 . As we can see immediately, in the top layer the membrane stresses are reduced and in the bottom layer we have stresses up to almost 7 kN/m .

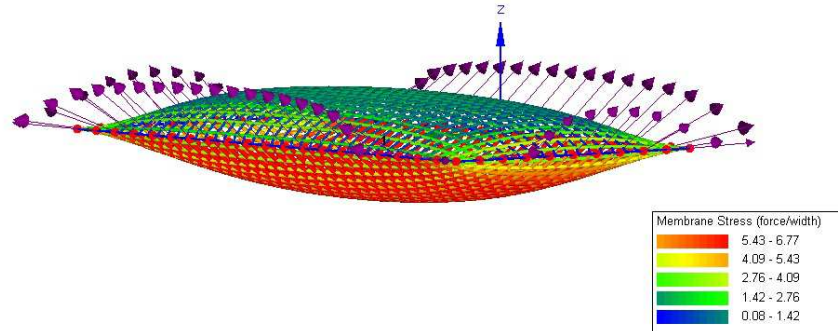


Figure 4: Cushion under snow loading

LC 2: Fast wind pressure. (steered by gas-law ($pV=constant$))

The wind pressure loads are only on the top-layer of the cushion. We assume the wind gust so fast, that the gas-law can be used. The operating pressure before wind loading is 0.35 kN/m^2 . It is increased by the gas-law to 0.45 kN/m^2 and the volume is decreased from 400 m^3 to 399.6 m^3 . The behavior in its quality is very similar to LC 1, but here the gas law is valid. The product form p_1 and V_1 before loading is identical to the product p_2 and V_2 under wind pressure loads. The gas law in our example is $(p_1 + p_0)V_1 = (p_2 + p_0)V_2$. We have to consider that in the gas law the absolute pressure and not the difference pressure is applied. In the gas law we always have to add the atmospheric pressure p_0 (100.0 kN/m^2) to the difference pressure (p_1 or p_2). With our number we get $100.35 * 400.0 = 100.45 * 399.6 = 40140$.

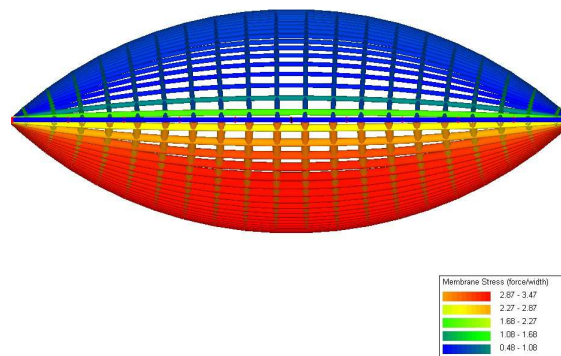


Figure 5: Cushion under wind pressure

LC 3: Fast wind overall suction. (steered by gas-law ($pV=constant$))

The wind loads are on the top and on the bottom layer of the cushion. The operating pressure is decreased from 0.35 kN/m^2 to -0.42 kN/m^2 and the volume is increased to 403.1 m^3 . In this example the gas law is very helpful; the membrane stresses remain moderate, because of the strongly decreased inner pressure (even to negative).

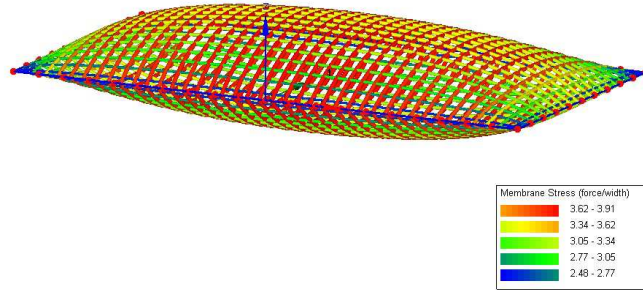


Figure 6: Cushion under wind suction

In our example the outer boundary was assumed to be fixed. But in reality we have a bending stiff frame with a specific stiffness or flexibility. In order to take these facts into consideration we have to extend our model by bending elements.

Beam Elements

The internal energy of beam element can be expressed in the already known form

$\frac{1}{2} \mathbf{v}^T \mathbf{R} \mathbf{v}$. Therefore we have to introduce angles being used for the formulation of

the inner energy. A bending element connects a start-point and an end-point. The angle between the direct line between start- and end-point and the direction of the real axis in the start point is called δv_{start} . On the end point we have the angle δv_{end} .

Those 2 angles are measured in the u, w -projection of the local coordinate-system, which is updated in each iteration. $\delta v_{sum} = \delta v_{start} + \delta v_{end}$ and

$\delta v_{dif} = \delta v_{start} - \delta v_{end}$. Analogue for the angles δw in the u, v -plane. For the

torsion we introduce an angle δu . This angle is found as follows: the 3D rotation of the starting-point with respect to the updated local coordinate system is executed with respect to v - and w -axis in the starting and ending point. The angle difference in the v, w -plane between starting and ending is called δu . The axial force is simple. The difference between stressed length l and unstressed length l_0 is measured. Now

the inner energy of one bending element can be written as $\sum_{i=1}^6 \frac{1}{2} v_i^2 r_i$ and more

detailed:

$$\begin{array}{ll}
v_{bendSv} &= \delta v_{sum} - \delta v 0_{sum} & r_{bendSv} &= 3EI_w l_0^{-1} \\
v_{bendDv} &= \delta v_{dif} - \delta v 0_{dif} & r_{bendDv} &= EI_w l_0^{-1} \\
v_{bendSw} &= \delta w_{sum} - \delta w 0_{sum} & r_{bendSw} &= 3EI_v l_0^{-1} \\
v_{bendDw} &= \delta w_{dif} - \delta w 0_{dif} & r_{bendDw} &= EI_v l_0^{-1} \\
v_{torsion} &= \delta u - \delta u 0 & r_{torsion} &= GI_t l_0^{-1} \\
v_{axial} &= l - l_0 & r_{axial} &= EAI_0^{-1}.
\end{array}$$

We change our system from the example by creating a free beam as boundary. In the LC snow we can see the bending moments (around v - and w -axis) in the beam-ring.

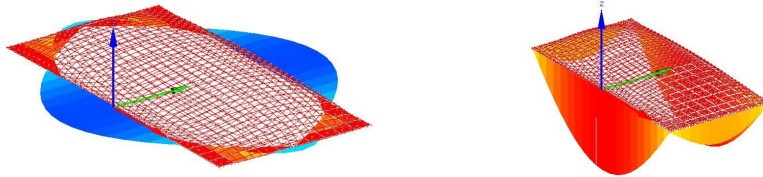


Figure 6: Cushion under wind suction

Example 2:

The Volume Formfinding example has a circular geometry with a diameter of 6 m . The required volume V_0 of the upper chamber is 12 m^3 and of the lower chamber 9 m^3 . With a desired stress distribution of 1 kN/m in both directions in all layers we end up with the result in Fig. 7.

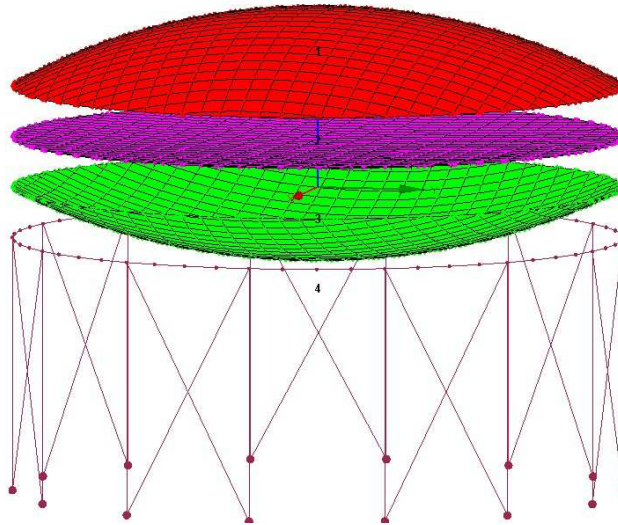


Figure 7: 2-chamber-cushion (exploded)

The upper chamber is defined by the red and violet triangles; the lower chamber by the violet and green triangles. We receive in the Volume Formfinding result an internal pressure of 0.33 kN/m^2 in the upper chamber, and 0.30 kN/m^2 in the lower chamber. In this example we want to put the focus onto the gas law within our theory: therefore we define in the first loadcase (LC1) a fast windgust (overall suction) and we maintain the operating pressures (0.33 and 0.30 kN/m^2). We assume in a second loadcase (LC 2) the gas-law to be valid; this means: the product from the absolute internal pressure with its volume remains constant during wind-loading.

LC 1: Fast wind overall suction: steered by internal pressure

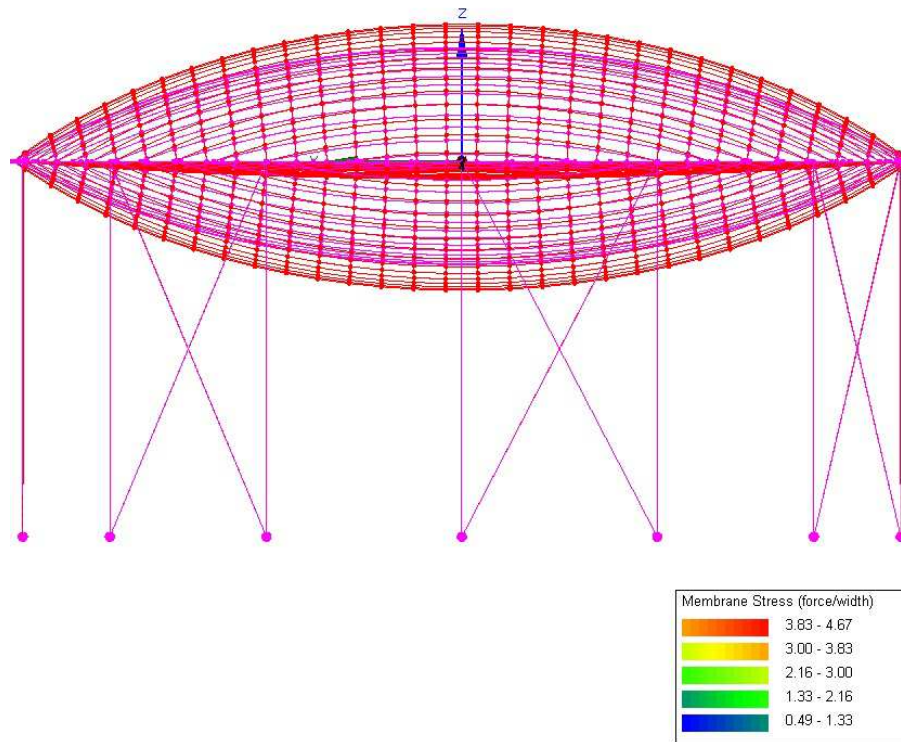


Figure 8: Large deflections and large membrane stresses

Here the membrane stresses are very high: the reason is simple; the constant internal pressure and the overall wind-suction have the same directions; the membrane is loaded by superimposed loads; therefore the stresses are up to almost 5 kN/m .

LC 2: Fast wind overall suction: steered by gas-law

Now the internal pressures are decreased; only -0.93 kN/m^2 in the upper chamber and -0.95 kN/m^2 in the lower chamber remain. The volumes increase to 12.135 m^3 in the upper and to 9.100 m^3 in the lower chamber. These facts are essential for the stresses: they are very moderate (approx. 1 kN/m).

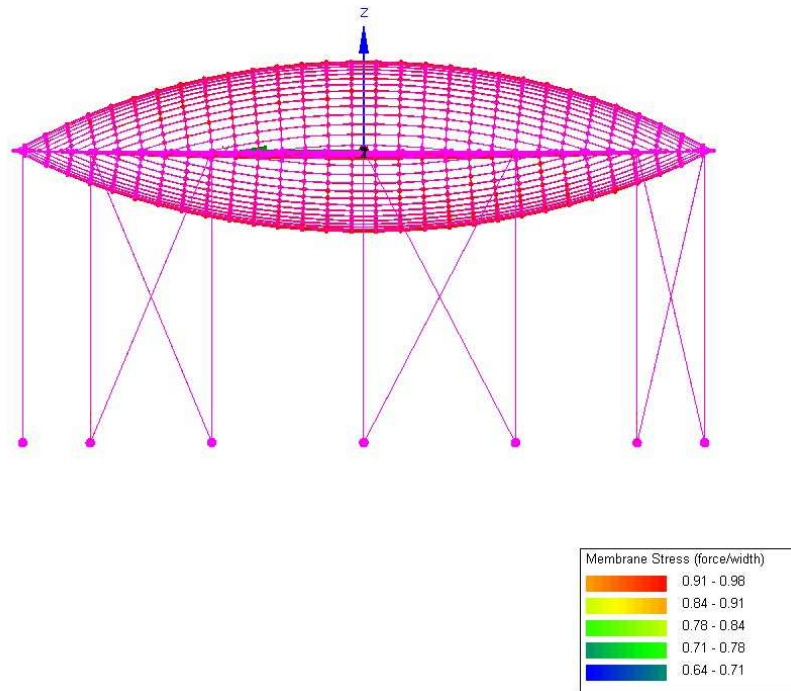


Figure 9: Small deflections and small membrane stresses

The combination of membrane-elements, cables, struts, beam-elements together with constraints as gas-law, constant inner pressure or volume in one or any number of chambers can be managed with the shown theory.

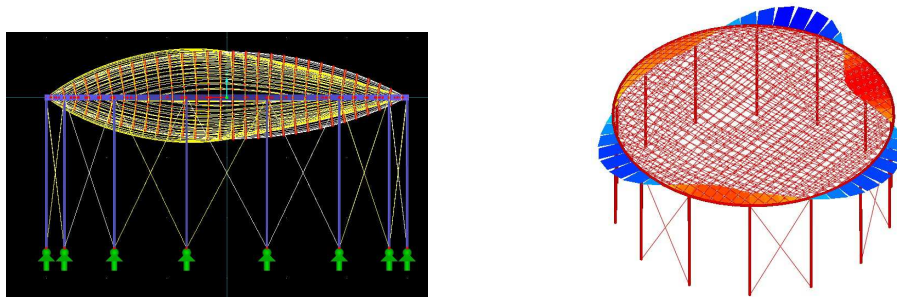


Figure 10: Deflections and internal moments

3 Cutting Patterns of Pneumatics

The calculation of cutting patterns should be done for all cushions but especially also for ETFE foils with highest accuracy. Cushions are mainly fixed by very non-flexible or very stiff boundaries. Therefore we have no chance to adjust an inaccurate patterning as we can do it in case of free boundaries (e.g. cables in a pocket) for mechanically stressed membranes. In order to avoid waste of material we have to adjust the maximum patterning widths to the role widths (or in whole-number parts of it). The maximum widths of cushion-patterns lie in ridge line. Therefore an automatic widths-optimisation is possible using this line as guide-line.

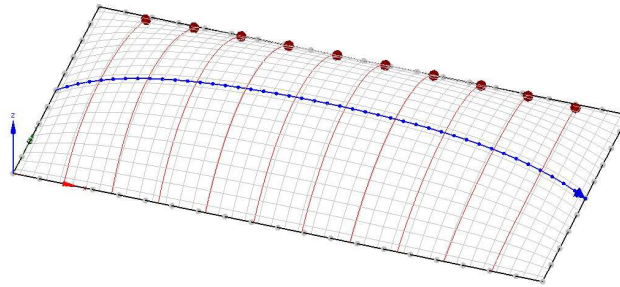


Figure 11: Cushion with geodesic lines

We simply generate points on this line having the distance of the desired cloth-widths. Now geodesic lines - which are perpendicular to the ridge-line - are produced automatically. Then the flattening procedure is executed: seam-allowances and welding marks are generated to simplify the whole production-line. Also quality numbers are calculated, they can be used to check if the widths are small enough to get well-stressed surfaces without any wrinkles. The non-compensated and adjusted boundary lines are absolutely as they have to be: 10.000 and 20.000 m. The area differences between 3D cushion-area and 2D patterns-area are smaller than 0.02% . So a wrinkle-free cushion is guaranteed.

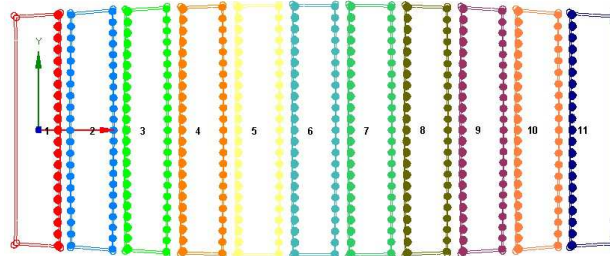


Figure 12: Flattened patterns

Often we have to consider in the patterning procedure for ETFE cushions, that the seams in the fixed boundaries from upper and lower layer are not at the same position. We support our clients by showing the seams e.g. from the upper layer

during the patterning procedure of the lower layer. So the gaps in between different layers can simply be managed.

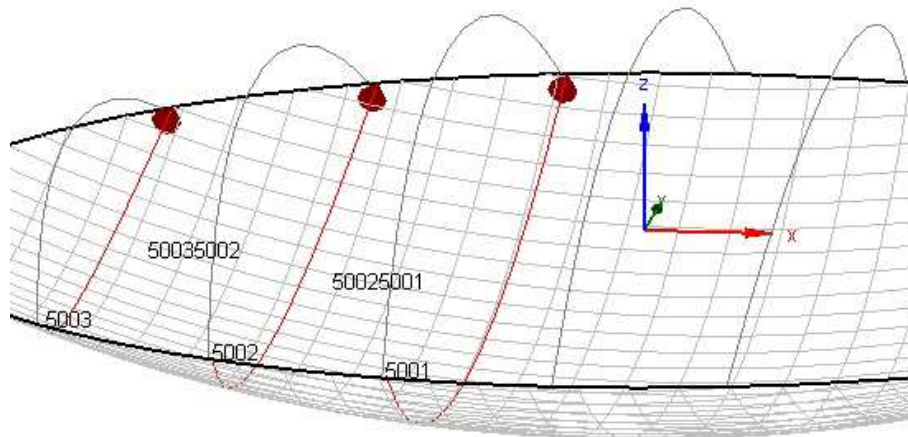


Figure 13: Gap optimisation

References

- [1] Linkwitz, K. and Schek, H.-J., (1971), 'Einige Bemerkungen zur Berechnung von vorgespannten Seilnetzkonstruktionen', *Ingenieur-Archiv* **40**, 145-158.
- [2] Schek, H.-J., (1974), 'The force density method for form finding and computation of general networks', *Computer Methods in Applied Mechanics and Engineering* **3**, 115-134.
- [3] Gründig, L., (1975), 'Die Berechnung von vorgespannten Seilnetzen und Hängenetzen unter Berücksichtigung ihrer topologischen und physikalischen Eigenschaften und der Ausgleichsrechnung', Dissertationsschrift, *DGK Reihe C*, Nr. 216, 1976 and *SFB 64-Mitteilungen* 34/1976.
- [4] Singer, P., (1995), 'Die Berechnung von Minimalflächen, Seifenblasen, Membrane und Pneus aus geodätischer Sicht', Dissertationsschrift, *DGK Reihe C*, Nr. 448, 1995.
- [5] Ströbel, D., (1997), 'Die Anwendung der Ausgleichsrechnung auf elastomechanische Systeme', *DGK, Reihe C*, Nr. 478.